THE JOURNAL OF CHEMICAL PHYSICS **143**, 204305 (2015)

Cold and ultracold dynamics of the barrierless $D^+ + H_2$ reaction: Quantum reactive calculations for $\sim R^{-4}$ long range interaction potentials

Manuel Lara,[1,a)] P. G. Jambrina,[2] F. J. Aoiz,[2] and J.-M. Launay[3]
[1]*Departamento de Química Física Aplicada, Facultad de Ciencias, Universidad Autónoma de Madrid, 28049 Madrid, Spain*
[2]*Departamento de Química Física, Facultad de Química, Universidad Complutense, 28040 Madrid, Spain*
[3]*Institut de Physique de Rennes, UMR CNRS 6251, Université de Rennes I, F-35042 Rennes, France*

(Received 9 September 2015; accepted 7 November 2015; published online 24 November 2015)

Quantum reactive and elastic cross sections and rate coefficients have been calculated for $D^+ + H_2$ ($v = 0$, $j = 0$) collisions in the energy range from 10^{-8} K (deep ultracold regime), where only one partial wave is open, to 150 K (Langevin regime) where many of them contribute. In systems involving ions, the $\sim R^{-4}$ behavior extends the interaction up to extremely long distances, requiring a special treatment. To this purpose, we have used a modified version of the hyperspherical quantum reactive scattering method, which allows the propagations up to distances of 10^5 a_0 needed to converge the elastic cross sections. Interpolation procedures are also proposed which may reduce the cost of exact dynamical calculations at such low energies. Calculations have been carried out on the PES by Velilla *et al.* [J. Chem. Phys. **129**, 084307 (2008)] which accurately reproduces the long range interactions. Results on its prequel, the PES by Aguado *et al.* [J. Chem. Phys. **112**, 1240 (2000)], are also shown in order to emphasize the significance of the inclusion of the long range interactions. The calculated reaction rate coefficient changes less than one order of magnitude in a collision energy range of ten orders of magnitude, and it is found in very good agreement with the available experimental data in the region where they exist (10-100 K). State-to-state reaction probabilities are also provided which show that for each partial wave, the distribution of HD final states remains essentially constant below 1 K. © *2015 AIP Publishing LLC.* [http://dx.doi.org/10.1063/1.4936144]

I. INTRODUCTION

The attention in the field of (ultra-)cold reaction dynamics has mainly focused in reactions involving alkali atoms and dimers, since (ultra-)cold samples of this species are relatively easy to produce.[1–7] However, new experimental approaches are changing this scenario, providing detailed information on more generic bimolecular systems at very low collision energies,[8–14] eventually bridging the gap between cold ($T < 1$ K) and ultracold ($T < 1$ mK) regimes.[15–19] While the availability of new experimental results calls for computational studies to be extended to the ultracold regime, advances in the theoretical simulation of these processes are hampered by the limitation in the accuracy of the state-of-the-art electronic calculations, typically larger than the collision energies involved. While for light atom+diatom systems, collision energies in the range of ~1 K lie within the limits of what is considered as predictable using conventional theoretical tools, "exact" quantum results at much lower energies can be always put into question.

Until recently, errors in *ab initio* PES were in the order of 1 kcal/mol, the so-called chemical accuracy. Given the high kinetic energies and the predominance of potential barriers, the effects of Short Range (SR) chemical interactions have constituted the main focus. It was pointless to attempt an accurate description of the much smaller interactions at the Long Range (LR). Distances as short as 20-30 a_0 were already considered as potential free regions. This was and still is a general practice in both time-dependent and time-independent methods in order to avoid long propagations at thermal energies. In more recent years, electronic structure calculations have become considerably more accurate and the limits of accuracy can be set on the order of 10 cm^{-1}.

Nevertheless, at low temperatures, larger accuracies are required. LR interactions are of the same order of magnitude as the small kinetic energies considered and thus cannot be neglected. Moreover, reactions that are studied at such low energies are typically barrierless where only the centrifugal barrier thwarts the reaction. Located at considerably large intermolecular distances, the width and the height of the centrifugal barrier are determined by the LR interactions. Indeed, the LR part of the potential is essential as it determines the amount of incoming flux which is able to reach the transition state region of the PES and thus to react. In this way, in the cold regime, both SR and LR interactions are important, and the use of a PES which describes accurately the whole configuration space is required.

At even lower energies, in the ultracold regime, the influence of the LR interactions becomes paramount, leading in extreme cases to the paradoxical idea of *universality*:[20] the result of the collision depends exclusively on the LR behavior and not on the SR chemical interactions. The ultracold regime is governed by Wigner laws[21] and can be described

a)Author to whom correspondence should be addressed. Electronic mail: manuel.lara@uam.es

in simple terms using the scattering length. The extreme sensitivity of this parameter to the details of the PES, and the combined action of the surface as a whole, makes extremely difficult to predict its value theoretically or, conversely, to deconvolute the underlying interactions from its measurement.

There are already some theoretical studies in the literature on atom + diatom neutral chemical reactions at cold and ultracold temperatures.[22,23] Although it is difficult to assess the accuracy of the calculations, they provide us with general trends in the behavior of such systems. However, very few works have focused on systems involving ions.[24–27] This is probably due to the presence of the $\sim R^{-4}$ potential term (instead of the common $\sim R^{-6}$), which extends the interaction up to extremely long distances in ionic systems, making very difficult to obtain converged results. Here, we will consider the benchmark ion-molecule barrierless reaction $D^+ + H_2 \rightarrow H^+ + HD$. We will show how to account for the $\sim R^{-4}$ LR behavior when calculating reactive and elastic cross sections and rate coefficients. As for the accuracy of the results, the same caveats as in similar works in the ultracold regime hold here. In the spirit of the seminal paper by Gribakin and Flambaum,[28] our study can be considered as an effort to unravel the "typical" scattering length that one may expect, even when small inaccuracies in the PES can make it fluctuate.

In many instances, reactions of ions with neutrals, such as the title reaction, are essentially barrierless and, due to their LR attractive potential, exhibit large cross sections. This renders them especially relevant at the low temperatures typical of the interstellar medium (see Refs. 29–31, and references therein). In the past decades, much experimental effort was dedicated to extend the temperature range down to a few K. The difficulties associated with the handling of small relative translational energies in ion–molecule reactions have been overcome through the use of supersonic jets,[32–35] guided and merged beams, and ion traps.[36–40] The flourishing technology of Coulomb crystals in radio frequency ion traps[41] and the possibility of combining them with traps for neutrals or with slow molecular beams[42,43] foresee a great progress in the experimental study of cold ion-neutral reactions. Recent experiments have been able to stabilize H_3^+, the strongly bound collision complex formed during the collision $H^+ + H_2$, for energies as low as 11 K in ion traps.[44] Indeed, experiments to determine low temperature state specific rate coefficients in the title system are within the reach of current radio frequency ion trap technology.

Due to its apparent simplicity, the H_3^+ system constitutes a prototype in the field of ion-molecule reactions. As a result of this, it has attracted great deal of attention from both theoreticians and experimentalists.

Early calculations starting in the seventies [45–49] disclosed the main characteristics of its mechanism that evolves from a low energy behavior, dominated by capture into a strongly interacting complex, to a higher energy behavior characterized by more direct collisions. Under these circumstances, shorter interaction times do not allow for a complete randomization of the energy, angular momentum, and nuclear scrambling within the reaction intermediate. The calculations, based on simple statistical models, semiempirical PESs, and a limited number of classical trajectories, were able to account reasonably well for the available experimental values of cross sections and rate coefficients,[37,50–54] although not without considerable discrepancies.

Over the last two decades, a great progress has been achieved in the construction of accurate potential surfaces for the H_3^+ system.[55–61] Specifically, the ARTSP PES by Aguado *et al.*[56] has proved to be one of the most accurate global PESs widely used over the last few years. More recently, this PES was modified by Velilla *et al.*[60] (hereinafter VLABP PES) in order to account for the LR interaction. In parallel to the electronic structure developments, a selection of theoretical methods of varying accuracy has been applied to the study of the $H^+ + H_2$ reaction dynamics.[62–76]

Of all the possible isotopic variants of the $H^+ + H_2$ reaction that of the deuteron with H_2 is exothermic due to the different zero-point energies (ZPEs) of reactants and products and hence is appropriate for its study at the cold and ultra-cold energy regimes.[77] The isotopic substitution makes possible to readily identify reactants and products by mass spectrometry or spectroscopic techniques. In addition, $D^+ + H_2$ can play an important role in the unusual deuterium fractionation observed in many cold space environments.[78–80]

Calculations for the $D^+ + H_2$ reaction have been carried out on the VLABP PES at energies slightly above the cold regime[81–83] using the hyperspherical quantum reactive scattering method.[84] However, the implementation used in Refs. 81–83, suitable for the study of thermal or hyperthermal reactions, faces problems at energies below 10 K,[81] and it cannot be used at ultracold temperatures. As it will be shown, some methodological changes in the hyperspherical method are required to carry out accurate calculations at cold and ultracold energies at a reasonable computational expense.[85]

In a very recent work,[86] we have communicated part of the results from an extensive quantum study on the reactive collision $D^+ + \textit{para}\text{-}H_2 \rightarrow H^+ + HD$ using the VLABP PES[60] at cold and ultracold energies. Quantum reactive and elastic cross sections and rate coefficients were calculated using a modified hyperspherical quantum reactive scattering method.[84,85] For the first time, quantum results were obtained at energies as low as 10^{-8} K for a system whose $\sim R^{-4}$ LR behavior implies propagations up to very large distances. To the best of our knowledge, no other work in the literature has attained so low energies in an atom+molecule system with such an extended LR.

In this work, we will provide more details on the methodology and the dynamical results. Besides, we will discuss how the cost of time independent quantum mechanical (TIQM) calculations can be considerably reduced by using interpolation techniques of the logarithmic derivative matrix. By comparing with the results obtained using the ARTSP PES, whose fitting does not explicitly include the LR behaviour in an analytical way, we will emphasize the significance of the inclusion of the LR interactions. We will propose a very simple model to improve Langevin type estimates for cross sections at low energies in complex-mediated barrierless reactions. Finally, we will discuss the behavior of the system in the ultracold regime through the analysis of final-state resolved cross sections and reaction probabilities. The paper

is structured as follows. In Sec. II, we will briefly describe the theoretical methodology, including the possibility of using interpolation procedures. We also provide details on the considered PES and the calculation of effective potentials. The results from the dynamical calculations and the models to understand them will be shown and discussed in Section III. Finally, a summary of the work and the conclusions will be given in Section IV.

II. THEORETICAL METHODS

A. Dynamical methodology

The hyperspherical quantum reactive scattering method developed by Launay and Dourneuf[84] has been widely used for thermal and hyperthermal reactive scattering.[87–90] In this method, the configuration space is divided into inner and outer regions by the definition of a matching hyper-radius, ρ_0, beyond which no inelastic or reactive transition may appreciably occur. The positions of the nuclei in the inner region are described in terms of Smith-Witten hyperspherical democratic coordinates. The internal basis built in these coordinates is particularly well suited for insertion reactions with very deep wells. The log-derivative matrix at a particular total energy, $Z(E,\rho)$, is propagated outwards on a single adiabatic PES. Its value at ρ_0, $Z(E,\rho_0)$, is matched to a set of suitable radial functions, called asymptotic functions (AFs), which provide the collision boundary conditions, to yield the scattering S-matrix. At thermal energies, the AFs are the familiar regular and irregular radial Bessel functions (transformed into hyperspherical coordinates). They account for the presence of a centrifugal potential at finite distances, avoiding to extend the calculation to very large distances where the centrifugal potential vanishes.

To study cold and ultracold collisions of alkalis, the AFs were modified to account for both the centrifugal and the isotropic R^{-6} LR potential.[90–92] More recently, these changes were generalized to allow the treatment of general anisotropic LR potentials:[85] the AFs are obtained numerically and they are adapted to the specific LR behavior of the system, ensuring the collisional boundary conditions while working at finite distance. This avoids propagations in hyperspherical coordinates up to extremely large intermolecular separations. The AFs are calculated by solving a system of radial differential equations in Jacobi coordinates[85] using the coupled-equation version of the method of De Vogelaere.[93] Very long propagations are required for their calculation, starting at large radial distances—where LR interactions are negligible—up to ρ_0. In any case, the expense is minimal in comparison with the propagation in hyperspherical coordinates. Such implementation is applied here to a system involving ions, with $\sim R^{-4}$ LR behavior. Let us note that to converge the partial elastic cross sections at a collision energy of 10^{-8} K, propagations starting at separations of 3×10^5 a_0 were needed. However, the computational cost of this calculation is affordable; furthermore, for the case $j = 0$, the number of coupled equations is reduced to one. Reaching so large intermolecular separations would be unfeasible by considering a sole propagation in hyperspherical coordinates.

B. The interpolation procedures

The implementation of the hyperspherical method in two regions, the inner region, using hyperspherical coordinates, and the outer region described in Jacobi coordinates using AFs (see Fig. 1), is very appropriate for interpolation procedures in the spirit of multi-quantum defect theory (MQDT)[94,95] that, to the best of our knowledge, have not been exploited in the field of conventional (non-MQDT) atom-molecule reaction dynamics. The value of the hyperradius that separates the two regions, ρ_0, has to be large enough such that there are not inelastic or reactive transitions for $\rho > \rho_0$. However, as the calculations in hyperspherical coordinates are very demanding, ρ_0 values as small as possible are preferred, what implies that the chosen ρ_0 has to be converged. For low collision energies, in general, the kinetic energy at the converged ρ_0 is large in comparison to the collision energy. The interpolation method is as follows.

Let us assume that we are running a set of QM propagations for a small range of energies $E \in [E_1, E_2]$, where $\Delta E = E_2 - E_1$. The propagation in the outer region, where LR interactions prevail, is likely to be extremely sensitive to small energy differences. However, the propagation in the inner region, where SR chemical forces prevail, may not fluctuate that much as long as the kinetic energy at ρ_0, $E_{\rm kin}(\rho_0)$, is essentially the same in the whole range of energies considered. In particular, if $\Delta E \ll E_{\rm kin}(\rho_0)$, it is expected that the log-derivative $Z(E,\rho_0)$ will barely change in the considered ΔE. In this way, the value $Z(E,\rho_0)$ for any energy in the interval can be calculated by interpolating the values at the endpoints, $Z(E_1,\rho_0)$ and $Z(E_2,\rho_0)$. The interpolated $Z(E,\rho_0)$ is then matched to the correct AFs in order to get the S matrix. Similarly, one could calculate $Z(E,\rho_0)$ for a sparse grid of energies, $E_1, E_2, \ldots$ in the desired range, and obtain the value for any other intermediate energy by linear or higher order interpolation.[94] These procedures may lead to a considerable reduction of the computational cost. For the title reaction, we have checked that using quadratic

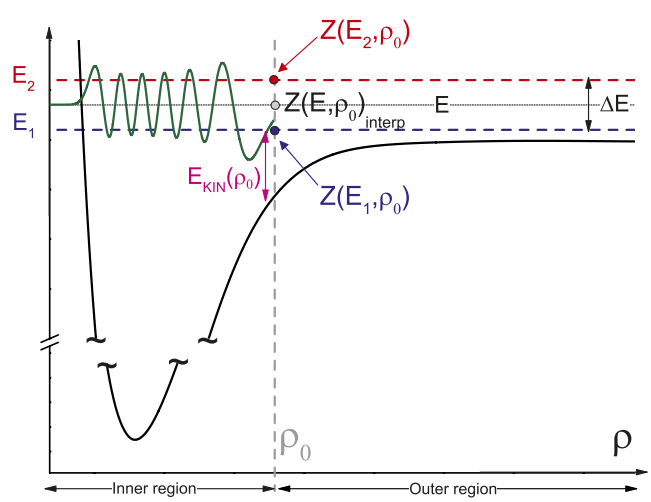

FIG. 1. Interpolation procedures can be used in order to get the logarithmic derivative at any collision energy, E, in the interval $[E_1, E_2]$, $Z(E,\rho_0)_{\rm interp}$, by starting from the logarithmic derivative at the endpoints $Z(E_1,\rho_0)$ and $Z(E_2,\rho_0)$.

(three-point) interpolation of the logarithmic derivatives obtained for $E_1 = 10^{-8}$ K, $E_2 = 0.1$ K, and $E_3 = 0.2$ K, we can successfully reproduce the cross section for any energy below 0.1 K, within relative errors $\leq 0.1\%$. Nevertheless, it must be emphasized that no interpolation procedure has been used in any of the results presented hereinafter.

C. Potential energy surface

At energies below 1.7 eV, such as those considered in this work, the only reactive process that can take place is the non-charge-transfer proton exchange process, and the reaction can be rigorously described using the ground adiabatic PES. The absence of any potential barrier, a deep well ($\approx$4.5 eV), and a small exoergicity (that of the difference of the zero point energies) are the main features of the PES. The energy of the $H_2(v = 0, j = 0)$ state is slightly larger than that of the $HD(v = 0, j = 2)$, so even at the lowest collision energies considered here, three product rovibrational states are accessible. The $HD(v = 0, j = 3)$ state has an internal energy above the largest total energy considered ($\approx$150 K) in this work and is closed.

Among the existing available PESs, the VLABP PES,[60] chosen in this work, is expected to fulfill our requirement for accuracy in both the SR and LR regions. LR interactions are included in the functional form of the potential. The asymptotic form of the PES in reactant Jacobi coordinates (r, R, θ) is given by

$$V_{\rm LR}(r,R,\theta) = Q_2(r)P_2(\cos\theta)R^{-3} - \left\{\frac{1}{2}\alpha_0(r) + \frac{1}{3}[\alpha_\parallel(r) - \alpha_\perp(r)]P_2(\cos\theta)\right\}R^{-4} + \cdots, \quad (1)$$

where $Q_2(r)$ is the quadrupole moment, and $\alpha_0(r)$, $\alpha_\parallel(r)$, and $\alpha_\perp(r)$ are, respectively, the isotropic, parallel, and perpendicular polarizabilities of H_2.[60] As Eq. (1) shows, the dominant contributions involve the charge-quadrupole interaction, varying as $\sim R^{-3}$, and the charge-induced dipole, varying as $\sim R^{-4}$.

To show the importance of LR effects, the results obtained by using the VLABP PES are compared with those obtained using its predecessor, the ARTSP PES.[56] The VLABP PES is a recent refinement of the ARTSP, based on the same set of *ab initio* points; however, the VLABP PES correctly accounts for the LR behavior while the ARTSP PES does not.

D. The effective potentials

If $\boldsymbol{\ell}$ labels the relative orbital angular momentum, and $\boldsymbol{j}$ the rotational angular momentum of H_2, the total angular momentum of the nuclei is given by $\boldsymbol{J} = \boldsymbol{j} + \boldsymbol{\ell}$. A convenient basis in order to expand the nuclear wavefunction in the LR region is the one characterized by quantum numbers (J, M, v, j, ℓ), represented as $\varphi^{JM}_{vj\ell}$, with (J, M) the total angular momentum and its projection on the Space-Fixed (SF) Z axis, (v, j) the rovibrational quantum numbers of the diatom and ℓ the relative orbital angular momentum. Let us consider the matrix of the electronic potential expressed in this basis,

$$V_{\ell\ell'}(R) = \langle \varphi^{JM}_{vj\ell} | V | \varphi^{JM}_{v'j'\ell'} \rangle, \quad (2)$$

where we will denote with primes other quantum states corresponding to the $H + D_2$ arrangement channel that can be coupled via the potential. The corresponding diagonal elements are useful in order to understand the dynamics because the diabatic effective potential felt by the colliding partners at a distance R when approaching in the state $\varphi^{JM}_{v_0j_0\ell_0}$ is given by

$$\langle \varphi^{JM}_{v_0j_0\ell_0} | V(R,r,\theta) | \varphi^{JM}_{v_0j_0\ell_0} \rangle + \frac{\ell_0(\ell_0+1)\hbar^2}{2\mu R^2}, \quad (3)$$

where $\langle \ldots \rangle$ indicates here the integration over the Jacobi coordinates r and θ.

To determine the potential matrix $V_{\ell,\ell'}(R)$, it is convenient to calculate first the matrix elements on the helicity basis, labeled by the projection Ω_j of $\boldsymbol{J}$ on the Body–Fixed (BF) coordinate system, whose z-axis is chosen along the reactant Jacobi $\boldsymbol{R}$ vector. This BF basis set is given by

$$\phi^{JM}_{vj\Omega_j} = \frac{\chi_{v,j}(r)}{r}\sqrt{\frac{2J+1}{4\pi}}D^{J*}_{M\Omega_j}(\alpha,\beta,\gamma)Y_{j\Omega_j}(\theta,0), \quad (4)$$

where $\chi_{v,j}(r)$ is the radial rovibrational wave function, $Y_{j\Omega_j}(\theta,\phi)$ the spherical harmonics, and $D^{J*}_{M\Omega_j}$ denotes a Wigner rotation matrix element with (α,β,γ) being the Euler angles corresponding to the transformation between SF and BF frames. The matrix elements of $V(R,r,\theta)$ are easily calculated in this basis using

$$V_{\Omega_j,\Omega'_j}(R) = \delta_{\Omega_j\Omega'_j} 2\pi \int \chi^2_{v,j}(r) Y^2_{j\Omega_j}(\theta,0) V(R,r,\theta)\sin\theta\, dr\, d\theta. \quad (5)$$

Once the potential matrix is known in the BF frame, we change to the SF basis (what involves a combination using $3j$ symbols) thus obtaining

$$V_{\ell,\ell'}(R) = (-1)^{\ell+\ell'}\sqrt{2\ell+1}\sqrt{2\ell'+1} \times \sum_{\Omega_j}\begin{pmatrix} j & \ell & J \\ \Omega_j & 0 & -\Omega_j \end{pmatrix}\begin{pmatrix} j & \ell' & J \\ \Omega_j & 0 & -\Omega_j \end{pmatrix} V_{\Omega_j,\Omega_j}(R). \quad (6)$$

We will limit our study to collisions with $H_2(v = 0, j = 0)$. For this particular case, the rotational wave function is the spherical harmonic Y_{00} ($\sim P_2$) and the integral in θ coordinate $\langle j = 0 | P_2(\cos\theta) | j = 0 \rangle$ is null. Thus, both the contributions from the charge-quadrupole and anisotropic polarization terms in Eq. (1) vanish, and although the asymptotic potential contains a $\sim R^{-3}$ term, the effective potential behaves as $-C_4/R^4$.

E. Classical Langevin model

The classical Langevin capture model for a R^{-4} potential is used to rationalize the cross sections and rate constants corresponding to ion + molecule collisions at thermal energies. This model is approximately valid for collisions dominated by attractive potentials and large reaction probabilities. It assumes a classical non-quantized orbital angular momentum and that

reaction takes place whenever the system is captured by the potential; if the kinetic energy is larger than the centrifugal barrier, the colliding partners are able to enter the inner part of the PES, and strongly interact, leading to reaction. Usually, this model gives the higher-limit to the reaction probability.

The Langevin expression for the reaction cross section, $\sigma_{\rm L}(E)$, and rate coefficient, $k_{\rm L}(E)$, can be obtained starting from the quantum expression

$$\sigma_r(E) = \sum_{\ell=0}^{\infty} \sigma_r^{\ell}(E) = (\pi/k^2) \sum_{\ell=0}^{\infty} (2\ell+1) P_r^{\ell}(E), \qquad (7)$$

where k is the wavenumber and $P_r^{\ell}(E)$ the reaction probability for a particular partial wave ℓ, by (i) calculating the centrifugal barrier height for each ℓ corresponding to an analytical potential $-C_4/R^4$; (ii) assuming that $P_r^{\ell}(E) = 1$ if the kinetic energy is higher than the centrifugal barrier, and null otherwise. (We will indistinctly use $P_r^{\ell}(E)$ or $P_r^{J}(E)$ in the notation below, as J and ℓ quantum numbers are equal for the particular case $j = 0$). With these approximations, the summation over ℓ is $(\ell_{\max}+1)^2$, where $\ell_{\max}$ is the maximum (integer) value of ℓ for which the kinetic energy is greater than the maximum of the effective potential. And finally, (iii) replacing the summation with an integral over continuous values of ℓ (valid for high enough values of ℓ), the cross section becomes $\sigma_r(E) = (\pi/k^2)\ell_{\max}(\ell_{\max}+1)$, where $\ell_{\max}$ is now a real number given by

$$\ell_{\max}(\ell_{\max}+1) = \frac{4\mu C_4^{1/2} E^{1/2}}{\hbar^2}. \qquad (8)$$

Hence, the resulting expression is the classical Langevin model cross section

$$\sigma_{\rm L}(E) = 2\pi (C_4/E)^{1/2}, \qquad (9)$$

and the Langevin rate coefficient

$$k_{\rm L}(E) = 2\pi (2C_4/\mu)^{1/2} \qquad (10)$$

which is independent on the temperature.

Notice the difference in the partial cross sections for continuous (classical Langevin deduction) and that assuming that the values of ℓ are discrete (integer) in the limit of ultracold temperatures. For $\ell = 0$ and assuming discrete values,

$$\sigma_r^{\ell=0}(E) = \frac{\pi}{k^2} \propto E^{-1} \qquad (11)$$

while for $\ell > 0$, $\sigma_r^{\ell} = 0$ at energies below the centrifugal barrier.

In contrast, for continuous values of ℓ, $\sigma_r(E) \propto E^{-1/2}$, regardless of the energy and the maximum value of ℓ. Therefore, with continuous values of ℓ, the result for a $n = 4$ potential *accidentally* coincides with the correct Wigner limit, as will be shown below.

A value of $C_4 = 2.70$ a.u. can be estimated according to the usual *ansatz* for ion-neutral interactions, $C_4 = \alpha_0 q^2/2$, where q is the charge of the ion (in a.u.) and α_0 the isotropic polarizability of the neutral atom or molecule ($\alpha_0 = 5.41$ a_0^3 (Ref. 96)). The value $C_4 = 2.71$ a.u., in excellent agreement with the former, can be extracted from the PES by equating the asymptotic effective potential for the $(J = 0, M = 0, v = 0, j = 0, l = 0)$ state to the expression $-C_4/R^4$. This latter value is the one we will consider below.

F. Numerical-capture statistical model

As it has been formulated, the Langevin model is a crude approximation. However, this model can be improved by (i) calculating the heights of the centrifugal barriers numerically, using the effective potentials, thus accounting for deviations from the R^{-4} behavior at short-range; (ii) carrying the summation over discrete partial waves instead of the integral; and (iii) correcting the assumption $P_r^{\ell}(E) = 1$ with a statistical factor to account for the fact that the probability of a complex to decompose into the products arrangement channel is lower than the unity. We will name this improved model "Numerical-Capture Statistical" model, in short NCS model. Note that when only $\ell = 0$ partial wave is open, this model predicts an $\sigma_r \propto E^{-1}$ behavior instead of the right Wigner limit.

The so-called "statistical factor" deserves more detailed comments. If the collision is assumed to be mediated by a complex, it is possible to decompose the whole collision process in two steps: the step of formation of the collision complex (capture) and the step of its dissociation. In complex mediated reactions with deep wells, the statistical *ansatz* can be applied: if there existed a complete loss of memory of the reacting flux within the complex, the break down of the complexes into fragments would be independent of the details of the initial state of the reagents which originated them (except for the total angular momentum and energy conservation). In that case (ergodic hypothesis), the total (summed over final states) reaction probability, $P_r^J(E)$, can be factorized as

$$P_r^J(E) \approx P_{\rm capt}^J(E) \times P_{\rightarrow \rm prod}^J(E), \qquad (12)$$

where $P_{\rm capt}^J(E)$ is the probability for the colliding partners to be captured in the complex and $P_{\rightarrow \rm prod}^J(E)$ is the probability to decompose, once the complex is formed, into products, i.e., what we have called *statistical factor*. When applied to a complex-mediated reaction, the assumption $P_r^J(E) = 1$ in the Langevin model is equivalent to a statistical factor of one, which is not generally true. An alternative value can be estimated by statistical means.

Within the statistical hypothesis, assuming total randomization inside the well, the fraction of complexes which decompose into the reactants ($D^+ + H_2$) or products ($H^+ + HD$) arrangements would be roughly proportional to the corresponding number of energetically accessible channels available from the complex, considering all of them as equiprobable. In particular, if we denote with $A(E)$ and $B(E)$ the number of energetically open channels corresponding to the reagent and product arrangements, respectively, the statistical factor may be approximated by $B(E)/(A(E)+B(E))$ (number of favored outcomes divided by the total number of equiprobable outcomes).[85] For any $J > 1$[97] (see note[106]), we find that $A(E) = 1$ and $B(E) = 6$, and one gets that $P_{\rightarrow \rm prod}^J(E) = 6/7 \approx 86\%$, which is the statistical factor we have used to correct the Langevin result. Only for $J = 0$ and $J = 1$, the fractions are different: $3/4 \approx 75\%$ and $5/6 \approx 83\%$, as it

corresponds to 3 and 5 open product channels (respectively) *versus* 1 open reactant channel. The factor 6/7 can be taken as an average statistical factor in the Langevin regime (where many partial waves are open) and is the factor we will use to correct the Langevin expression for the fraction of formed complexes which really decompose into the products. Let us note that whenever $B(E) \gg A(E)$, $P_{\rightarrow \mathrm{prod}}(E)^J \approx 1$, and the result would be equivalent to the Langevin assumption. This simple reasoning, just counting states, can be put in more solid grounds by making use of statistical models,[98] in their quantum,[97] or quasiclassical versions[99] which have been applied in the past to the H_3^+ system at thermal energies. They relate the fraction of complexes which decompose into a particular channel to the *capture* probability of forming the complex starting from it. In our simple procedure, we were assuming capture probabilities of 1 for the reactant and product states energetically accessible, what has sense if we are not extremely close to threshold; indeed, for attractive potentials in the absence of internal barriers, a few kelvin over threshold is enough.

III. RESULTS AND DISCUSSION

We have calculated quantum reactive cross sections and rate coefficients for $D^+ + H_2(v = 0,\ j = 0) \rightarrow H^+ + HD$ in the collision energy range 10^{-8}–150 K. Partial waves J = 0-17 were needed in order to converge the reactive cross sections in such range. The elastic counterparts require higher total angular momenta and they are only converged in partial waves up to approximately 1 K. The number of adiabatic channels in hyperspherical coordinates included in the calculations lies in the range from 200 to 1885, which correspond to $J = 0$ and $J = 17$, respectively. The propagation in hyperspherical coordinates was taken from $\rho = 0.5$ a$_0$ up to $\rho_0 = 35$ a$_0$, where the matching to the AFs was performed. In turn, the integration to calculate the AFs corresponding to the incoming channel at each considered energy was taken from a radial distance where the potential is 10^8 times smaller than the collision energy up to ρ_0. As noted above, this amounts to 3×10^5 a$_0$ for the lowest considered energy. Such a stringent criterion is found necessary in order to obtain the correct Wigner behavior of the partial elastic cross sections.

The considered energy range covers part of the thermal or Langevin regime, where an appreciable number of partial waves is open and the classical Langevin capture model may approximately work, and the cold ($T < 1$ K) and ultracold ($T < 1$ mK) regimes. We will discuss each region separately.

A. The reaction in the Langevin regime

In general, the applicability of the Langevin expression implies the concurrence of high enough partial waves.[100] At the energies explored in this work, the Langevin regime can be considered as spanning the 1-150 K range, with 5 and 17 partial waves open at 1 K and 150 K, respectively. The reaction cross sections obtained in this region are shown in the upper panel of Fig. 2. Results on the VLABP PES are compared

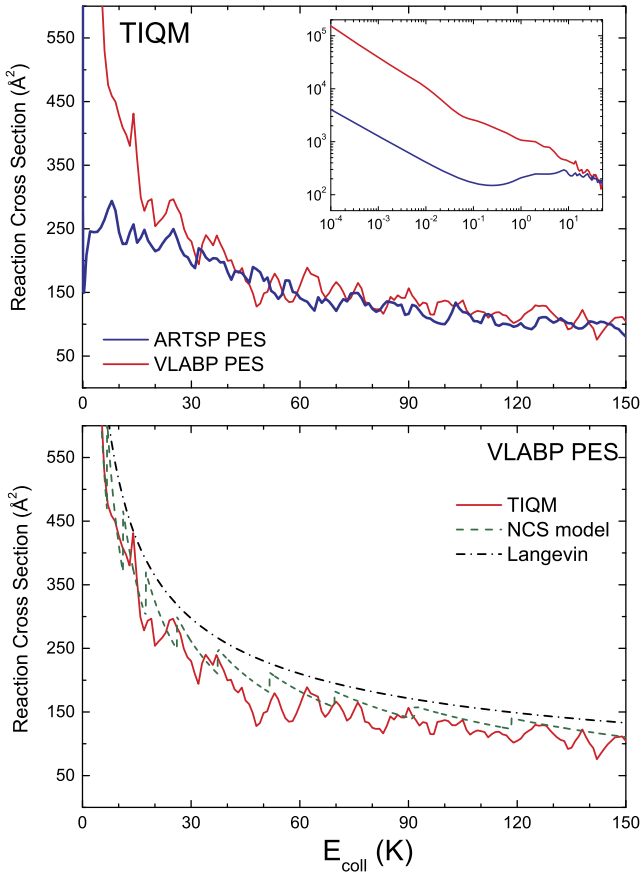

FIG. 2. Reaction cross sections for $D^+ + H_2$ ($v = 0$, $j = 0$) at collision energies in the Langevin regime. Upper panel: Comparison of the results calculated on the two considered PESs. The ARTSP PES is somewhat less reactive than the VLABP PES. The inset displays the cross sections for both PESs in the cold and ultracold regimes in logarithmic scale. The lower panel shows the comparison between the QM cross sections calculated using the VLABP PES with those obtained using the classical Langevin formula, Eq. (9), and the more realistic numerical-capture statistical model.

with the ones obtained using its precursor, the ARTSP PES, which does not account correctly for the LR interactions.

The inclusion of the $\sim R^{-4}$ LR term has led to significant changes in the cross section and, as expected, the role of the LR interactions is crucial at low collision energies. On average, the VLABP PES is somewhat more reactive than the ARTSP below 80 K, especially below 20 K. In the cold and ultracold regimes (see the inset in the upper panel of Fig. 2), the situation is critical, and the cross section calculated on the VLABP PES reaches a value forty times larger than that on the ARTSP PES. Of course, at such low energies, care should be exercised when comparing with a PES whose LR behavior is poorly described.

The lower panel of the Fig. 2 shows a comparison between the QM cross section calculated on the VLABP PES and that obtained using the Langevin and the NCS model. While the Langevin model overestimates the reactivity, there is a better agreement between the NCS model and our QM results. The sharp structures in the NCS model cross sections reflect the opening of partial waves and are located almost in coincidence with some of the peaks that survive the J averaging of the QM cross section. Most of the QM fine-grid structure, however,

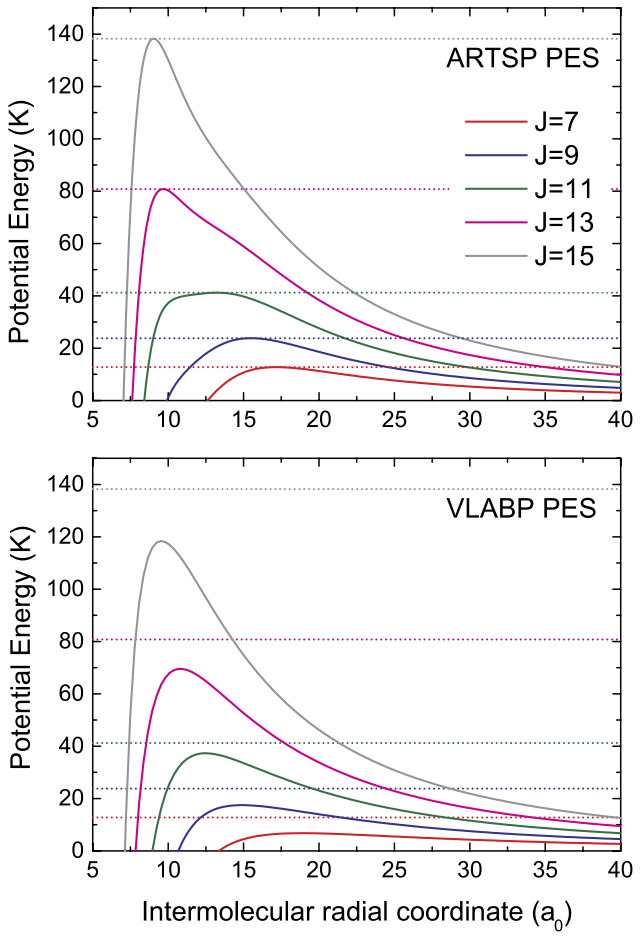

FIG. 3. The effective potentials (centrifugal plus attractive potential) for both PESs. The horizontal lines correspond to the maxima of the effective potentials on the ARTSP PES. The centrifugal barriers are lower in the case of the VLABP PES, which explains the higher reactivity observed at low energies.

cannot be explained in terms of the opening of additional partial-waves and can be attributed to resonances.

In order to understand the differences in reactivity between the two surfaces, we have calculated the effective potentials associated to some of the higher partial waves considered. These results are displayed in Fig. 3. As can be observed, the effective (potential plus centrifugal) barriers are significantly lower for the VLABP PES than for the ARTSP PES, and this fact explains the higher reactivity on the former PES. The polarization term, accurately included in the VLABP PES, makes the potential more attractive and pulls the effective potential down, thus allowing more incoming flux to reach the inner region where reaction may occur. Consistently, the reaction probabilities as a function of the energy for a given J on the ARTSP PES exhibit larger thresholds, as shown in Fig. 4. The height of the respective effective barriers for each value of J is indicated with vertical red and blue dotted lines for the VLABP and ARTSP potentials, respectively. Those would be the values of the reaction threshold in the absence of tunneling. However, tunneling across the effective barrier is relevant in all the cases and becomes more important with increasing J. This fact can be explained in terms of the decreasing width of the barriers with increasing J, as shown in Fig. 3. It is worth noticing that in some cases, tunneling is greatly enhanced by resonances just below the thresholds, as is the case for $J = 15$ on both PESs (Fig. 4). In addition, there is a dense resonance structure above threshold.

Reaction probabilities as a function of J (opacity functions) at four different kinetic energies, $E_{\rm coll} = 13$, 24, 41, and 81 K are shown in Fig. 5. For small values of J and leaving aside the resonance pattern, results on both PES are remarkably similar. However, for the largest values of J, in accordance with the effective potentials, the VLABP PES is somewhat more reactive. The differences are smaller with increasing collision energies as the effect of LR interactions is less significant and results on both PESs tend to converge. At the four energies considered, the maximum value of J that would be open neglecting tunneling, $J_{\rm max}$, is the same for both PESs, and the NCS results, which are thus also the same, are shown for the sake of comparison. Apart from the quantum oscillations, they are found to be in a reasonable agreement with the QM results. At the four energies studied, tunneling across the centrifugal barrier becomes evident and seems to be more important on the VLABP PES. From this comparison, we can easily conclude the need of a good description of the LR interactions when working at low collision energies, even for energies well above the cold regime.

In Fig. 6, the quantum specific rate coefficients (the cross sections multiplied by the relative velocity), $k(E)$, on the VLBAP PES are compared with the experimental results from Ref. 37. The agreement is fairly good, even though the experiments include the contribution from *ortho*-H_2, which is three times more abundant than *para*-H_2 in the experiment. Actually, the cross sections for $j = 0$ and $j = 1$ are not expected to be very different according to recent theoretical results.[83] The simple procedure of counting states leads to a statistical factor equal to 3/4 for the initial state $H_2(j = 1)$, very similar to the 6/7 corresponding to $j = 0$. It is worth noticing that 3/4 is precisely the ratio between the experimental cross sections in Ref. 37 and the pure Langevin value.

B. Low partial waves in the (ultra)cold regime

In the analysis of the (ultra)cold regime for a LR potential behaving as $-C_n/R^n$ $(n > 3)$, it is convenient to define the characteristic length, $R_n = (2\mu C_n/\hbar^2)^{1/(n-2)}$, and the characteristic energy, $E_n = \hbar^2/(2\mu R_n^2)$. The latter is of the order of the p-wave centrifugal barrier, which appears around R_n. For the case of $n = 4$, E_4 actually coincides with the height of the centrifugal barrier assuming that R_n is large enough for a $-C_4/R^4$ asymptotic behavior to be valid. It also coincides with the so-called mean scattering length $\bar{a}$.[28] In our system, $R_4 = \bar{a} \approx 99.7$ a$_0$ and $E_4 \approx 8.6 \times 10^{-3}$ K.[86]

The behavior of the cross sections at very low kinetic energies is given by the well known Wigner threshold laws,[21,101] which state that the elastic, $\sigma_{\rm el}^{\ell}$, and the total-loss (non-elastic) cross section, $\sigma_{\rm loss}^{\ell}$, associated to each partial wave varies close to threshold as

$$\sigma_{\rm el}^{\ell} \sim E^{2\ell}, \tag{13}$$

$$\sigma_{\rm loss}^{\ell} \sim E^{\ell-1/2}. \tag{14}$$

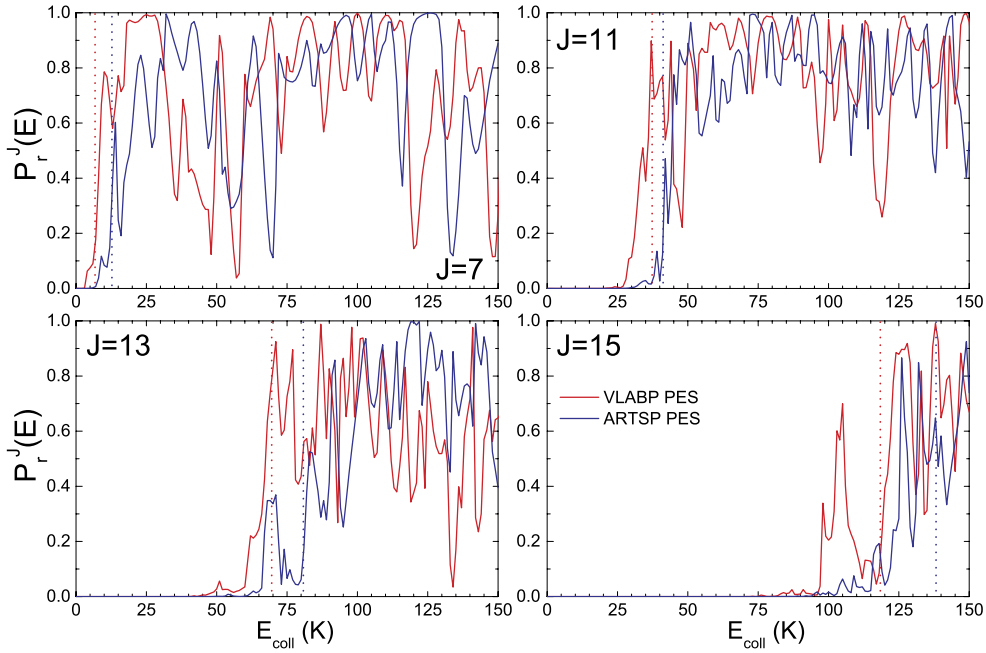

FIG. 4. Reaction probabilities as a function of the energy, $P_r^J(E)$, for $J = 7$, 11, 13, and 15 calculated on the VLABP PES (red lines) and on the ARTSP PES (blue lines). The position of the red and blue dashed vertical lines show the height of the effective potentials for VLABP and ARTSP PESs, respectively.

Nevertheless, the threshold laws for elastic scattering are modified for a potential with $n = 4$.[21,101] The phase shift for $\ell > 0$ at very low collision energies is dominated by a term $\sim E$ originating from the polarization potential.[102] Hence, the anomalous behavior of the elastic cross section is given by

$$\sigma_{\rm el}^0 \sim \text{constant}, \tag{15}$$

$$\sigma_{\rm el}^\ell \sim E \quad \text{for } \ell > 0. \tag{16}$$

In summary, while the partial reaction cross sections are expected to change as $E^{\ell-1/2}$, the partial elastic cross section will remain constant for $\ell = 0$, while changing as E for $\ell > 0$.

Given that $H_2(v = 0,\ j = 0)$ is the only rovibrational state of the reactants open at the considered energies, the inelastic process is absent and losses are only associated to reaction, $\sigma_{\rm loss}^\ell = \sigma_{\rm r}^\ell$. As long as one is not interested on product-state resolved magnitudes, it must be stressed that all the information is contained in the diagonal elements $S_{\ell m,\ell m}(k)$,

$$\sigma_{\rm el} = \sum_{\ell,m} \sigma_{\rm el}^{\ell m} = \frac{\pi}{k^2} \sum_{\ell m} |1 - S_{\ell m,\ell m}(k)|^2, \tag{17}$$

$$\sigma_{\rm r} = \sum_{\ell,m} \sigma_{\rm r}^{\ell m} = \frac{\pi}{k^2} \sum_{\ell m} [1 - |S_{\ell m,\ell m}(k)|^2]. \tag{18}$$

The expected behaviors can be distinguished in the left panels of Fig. 7, where the ultracold reaction and elastic cross sections calculated on the VLABP PES, for the lowest four partial waves, are shown in logarithmic scale. Note the change of slope of the reactive $J = 1(= \ell)$ p-wave at energies around E_4 (8.6 mK). It is also remarkable the anomalous behavior for $\sigma_{\rm el}^\ell$, with the slope of the elastic cross sections being the same

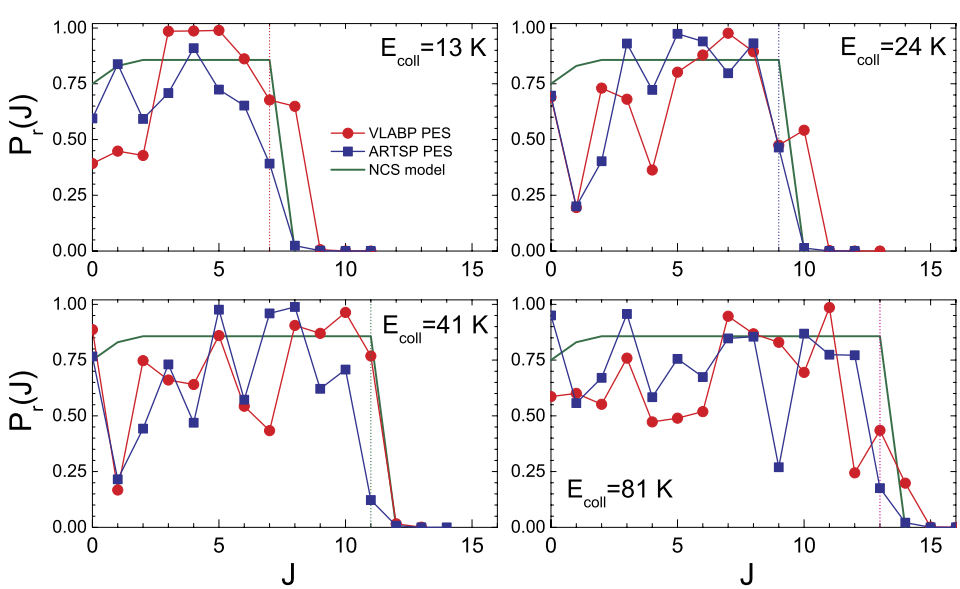

FIG. 5. Reaction probabilities as a function of J at four collision energies ($E_{\rm coll}$ = 13 K, 24 K, 41 K, and 81 K) for VLABP (red circles) and ARTSP PES (blue squares). At each of the energies here considered, the maximum value of J that would be open neglecting tunneling, $J_{\rm max}$, is the same for both PESs, and is shown using a vertical line. The $P_r(J)$ calculated according to the NCS model are also displayed (solid green lines).

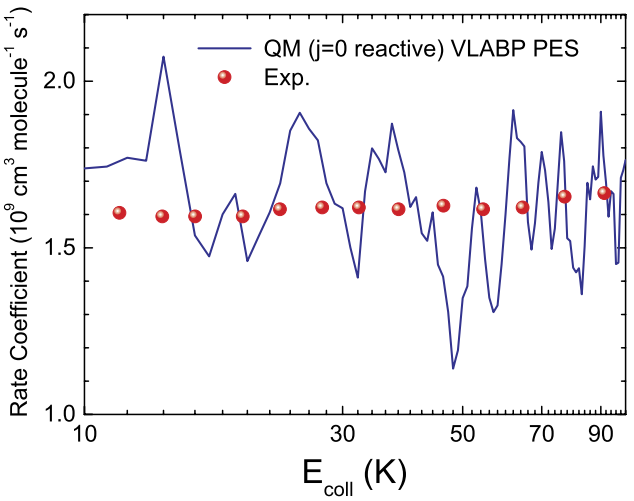

FIG. 6. Quantum specific rate coefficients calculated on the VLBAP PES (blue lines) compared with the experimental rate coefficients from Ref. 37 (red circles).

for any $\ell > 0$. Given the behaviors expected for $\ell = 0$, the total reaction cross section should change as $E^{-1/2}$ (the reaction rate coefficient being thus constant) and the total elastic cross section remain constant (the elastic rate coefficient changing as $E^{1/2}$) in the limit of extremely low kinetic energies, where only $\ell = 0$ is open (see, for example, total reaction and elastic rate coefficients shown in Fig. 8, which is discussed below). Interestingly, when the partial elastic cross sections are calculated on the ARTSP PES (bottom–right panel of Fig. 7) their slope is different for any $\ell > 1$, in clear contradiction with the expected threshold behavior for a $n = 4$ potential. This can be taken as an indication that a particular surface, the ARTPS surface in this case, is not reliable to describe low energy collisions.

To obtain information about the energy partition after the collision, we have calculated the state-to-state reaction cross sections (Fig. 9). Not only the total reactive cross sections follows the Wigner threshold law ($\sigma_r \propto E^{-1/2}$) but also the state-to-state cross sections do. Furthermore, for energies below 10^{-4} K, the $\sigma_r(j')/\sum_{j'}\sigma_r(j')$ ratio seems to remain constant. However, while $j' = 0$ is the highest populated state at the lowest energies, it is clearly less populated than $j' = 1$ and 2 for energies above 10 mK. Further information can be obtained resorting to the state-to-state reaction probabilities. In Fig. 10, their relative value to the overall reaction probability, $\overline{P}_r^J(j')$, is shown, where

$$\overline{P}_r^J(j') = \frac{P_r^J(j')}{\sum_{j'} P_r^J(j')} \tag{19}$$

and the summation runs over all the product channels. This ratio is preferred to the reaction probabilities *per se* because in contrast to the latter, which vanishes in the limit of zero kinetic energy, the former remains constant. Indeed, according to the factorization given by the statistical *ansatz* in Eq. (12), the dependence on the capture probability in numerator and denominator has to be cancelled. The capture probability, which would die as k in the limit of zero kinetic energy in order to fulfill the threshold law[107] would be the responsible for the individual reaction probabilities vanishing. Besides, and according to our simplistic approach to the statistical model, the ratio would remain constant and given by the quotient of the number of open channels corresponding to such rotational

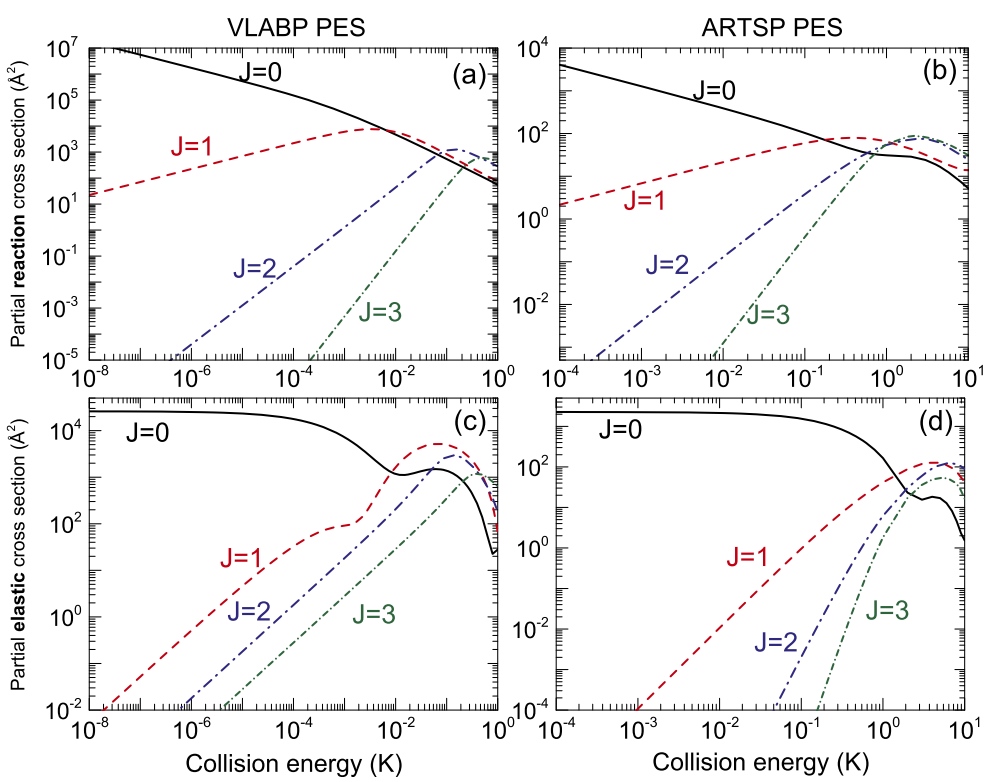

FIG. 7. Reaction and elastic partial cross sections corresponding to the lowest partial waves for $D^+ + H_2$ ($v = 0$, $j = 0$) collisions in the cold and ultracold regimes. Note that the scales of left and right panels are different.

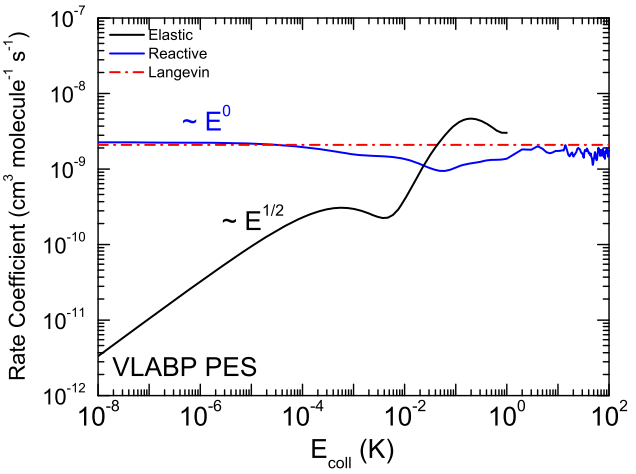

FIG. 8. Reaction (blue line) and elastic (black lines) rate coefficients for the collision $D^+ + H_2$ ($v = 0$, $j = 0$) on the VLABP PES. The Langevin reaction rate coefficient, given by Eq. (10), is also shown as a red dashed-dotted line. The comparison with the experimental of Ref. 37 in the 10-100 K range is shown in Fig. 6.

state and the total number of open channels. Indeed, roughly below 1 K (cold and ultracold energies) and regardless of the value of J, the $\overline{P}_r^J(j')$ and thus the distribution of internal states for each partial wave, remain constant. In contrast, they are governed by a dense oscillating pattern above 1 K (Langevin regime).

Focusing on the cold regime, for $J = 0$, most of the reactive flux goes to $j' = 0$ state, followed by $j' = 1$ and $j' = 2$. For $J = 1$, that trend changes and $j' = 1$ is more populated than $j' = 2$ and 0. Finally, for $J \geq 2$, $j' = 2$ is the most populated, followed by $j' = 1$ and 0. This trend can be rationalized in statistical terms. For $J = 0$, regardless of j', there is only one open channel for each HD rotational state — with quantum numbers ($v' = 0$, j', $\Omega'_j = 0$, $J = 0$) in a body-fixed basis or ($v' = 0$, j', $\ell' = j'$, $J = 0$) in a space-fixed basis — and the statistical reasoning predicts the same probability irrespective of j' for $J = 0$. Although similar, the quantum results show that there is some preference for small values of ℓ' so that $j' = 0$ gets more populated. For $J = 1$, the populations for $j' = 0$, 1, and 2 should keep the ratios 1:2:2, according to the open number of channels. Indeed, $j' = 1$ has a population around 40%, but the population for $j' = 0$ is somewhat too high and the one for $j' = 2$ is too low. Finally, for $J \geq 2$, there are three $j' = 2$ channels, two $j' = 1$ channels, and one $j' = 0$ channel, leading to $P_r^J(j' = 2) > P_r^J(j' = 1) > P_r^J(j' = 0)$. This crude statistical reasoning, based in the number of projections of j', is in agreement with the lower population of $j' = 0$, at energies above 10 mK, as found in Fig. 9.

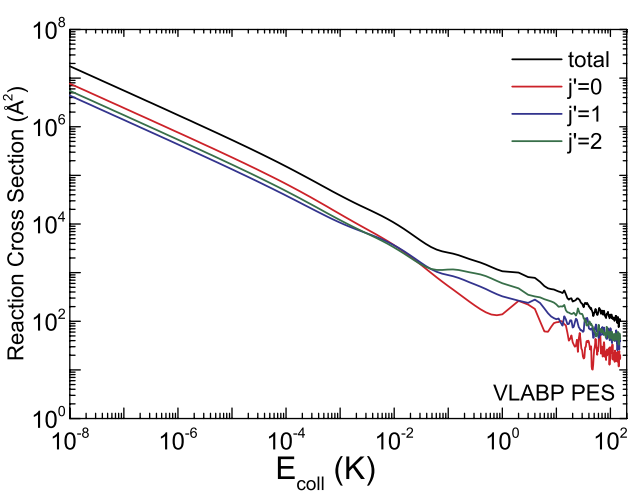

FIG. 9. State resolved reaction cross section for the collision $D^+ + H_2$ ($v = 0$, $j = 0$) $\rightarrow$ HD($v' = 0$, j') + H^+ on the VLABP PES.

C. The quantum Langevin behavior

It must be stressed again that the energy dependence of the Langevin model $\sigma_L(E)$, which should be valid only for high energies (when many partial waves are open), meets the requirements of Wigner threshold law ($\sigma_L(E) \sim E^{-1/2}$) in the zero collision energy limit. Such situation only occurs for the $n = 4$ case; for $n \neq 4$, the collision energy dependence of the Langevin cross section is not any longer $E^{-1/2}$. Therefore, for a $n = 4$ asymptotic potential, both the Langevin model at high energy and the Wigner threshold law in the ultracold regime predict energy independent reaction rate coefficients. Notably, this does not imply that their values must be coincident. However, the calculations show that in the present case, the ultracold rate coefficient is just ≈1.1 times bigger than that given by the Langevin model. Considering that in the high energy range, the rate coefficients are well accounted for by the latter model, it turns out that the reaction rate changes less than a factor of ten in a ten orders of magnitude energy range. Averaging over the Boltzmann distribution would surely make differences smaller. Hence, if confirmed by experimental measurement, it would result of a basically constant thermal rate coefficient. In what follows, we will try to rationalize this unexpected Langevin behavior at ultracold energies, where the centrifugal barrier does not even exist.

Very recently, and starting from slightly different quantum defect theory frameworks, two *quantal versions* of the Langevin model have been proposed.[103,104] These universal models (in the sense of an exclusive dependence on the LR) allow to change smoothly from the high energy regime to the ultracold region under the same Langevin assumption: all the flux reaching the short-range region leads to reaction. Or translated into the language of the model in Ref. 103, the one we will consider below: the loss probability at SR, P^{re}, is the unity. P^{re}, the flux that is irreversibly lost from the incoming channel at SR, is not directly observable nor necessarily coincides with the reaction probability $P_r^J(E)$. In very simplistic terms, the incoming flux which leads to reaction, $P_r^J(E)$, has to overcome two obstacles: (i) it needs to reach the SR region (without being reflected by the LR potential or the centrifugal barrier); (ii) it has to find its way to the products arrangements from the SR region. The latter process is precisely the one described by the P^{re} parameter. Only at high energies, in the absence of tunneling through the centrifugal barrier and when quantum reflection by the LR potential is negligible, we can affirm that $P_r^J(E) \approx P^{re}$. Furthermore, the expression

$$\sigma_r(E) \approx P^{re} \cdot \sigma_L(E) \tag{20}$$

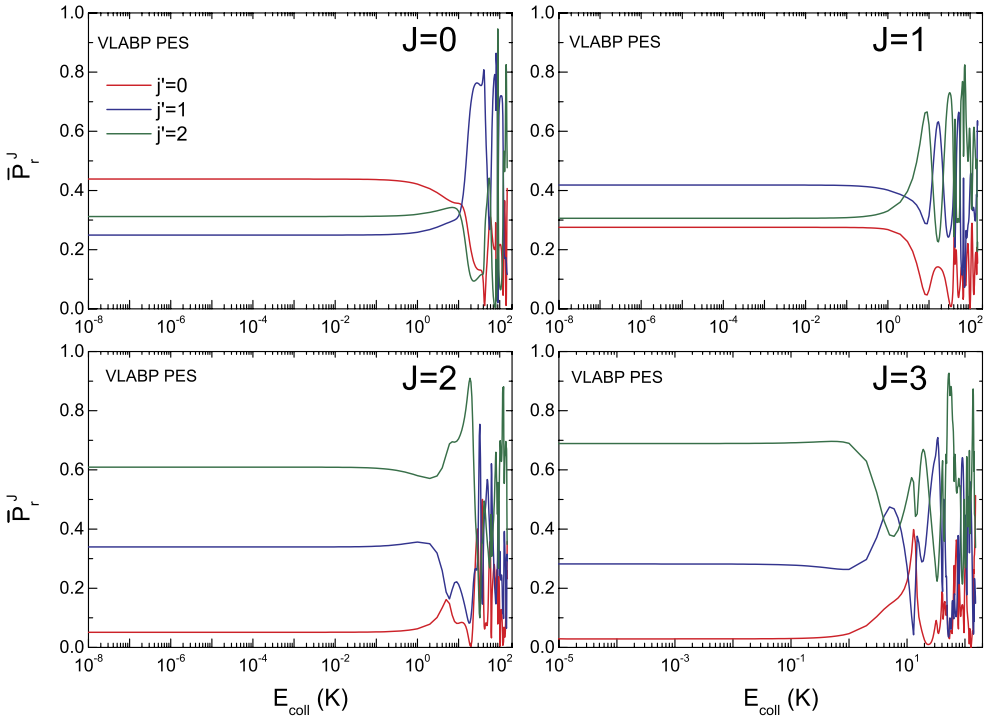

FIG. 10. Relative rotational state resolved reaction probability, $P_r^J(j')/\sum_{j'}P_r^J(j')$, for the collision $D^+ + H_2$ ($v = 0$, $j = 0$) on the VLABP PES.

should be valid in the Langevin regime if P^{re} is weakly dependent on the energy and the partial wave.[103]

Rather surprisingly, the conclusion derived from these models for $n = 4$, under the Langevin assumption ($P^{re} = 1$), is that the reaction cross section should reach a value $2\sigma_L(E)$, as will be elaborated below, in the limit of zero kinetic energy. This is twice the value predicted by the Langevin expression, and not simply $\sigma_L(E)$, which is what we have essentially got in the Wigner regime. To the extent that the model could be applied to the system, we can conclude that our system is not universal. That is, the SR interactions play a role and the probability to react once attained the transition state is not simply one.

This result was not unforeseen. The universal case ($P^{re} = 1$) is expected when the number of product states is large enough that all the reactive flux is irreversibly lost from the incident channel due to couplings. Nevertheless, this is probably not the case for the title reaction. There are many channels coupled to the initial one inside the well, and the randomization is equivalent to the population of all of them in the complex. However, there are only four open channels at the considered energies for $J = 0$, three of them corresponding to products. This makes reasonable the possibility of about 1/4 of the flux at SR trying to return from the complex to the incident channel, and thus $P^{re} \approx 3/4$. It can be argued that this estimate should be corrected: in order to reach the asymptotic region of the reactant channel, this flux has to traverse again the LR potential and part of it may be quantum reflected back into the well; however, these processes of transmission/reflection through the LR potential are not accounted for by the P^{re} parameter, but by the combination of the latter with the s parameter (see below). We can get another estimate for P^{re} from our quantum results. The relation $P_r^{J=0}(E) \approx P^{re}$ is expected to hold above the cold regime, when quantum reflection effects are negligible. If we average $P_r^{J=0}(E)$ (in order to eliminate energy dependent details) in the range 1-150 K, the value 0.58 results. However, it may be preferable to use the values for $\sigma_r(E)$, which is a more averaged quantity than the individual reaction probabilities, in order to get an *effective* value for P^{re} to characterize the reactive behaviour of the PES. Using Eq. (20) to fit our quantum results in the Langevin region, we find that $\sigma_r(E)/\sigma_L(E)$ has an average value of ≈0.8 in the range 1-150 K.[86]

The value we have obtained for the quantum rate at threshold, $k(E) \approx 1.1k_L$, is expected to be very sensitive to small inaccuracies in the PES. In contrast, our estimate for P^{re}, obtained by fitting the QM results in the Langevin region, where they are supposed to be almost quantitative, is expected to be more robust. Using this estimate, we will try to go further in our predictions regarding the ultracold regime. However, we need to delve more into the quantum defect model. According to it, the behavior in the Wigner limit depends on two parameters y and s. The first parameter, $0 \le y \le 1$, is directly connected to P^{re} through the equation

$$P^{re} = 4y/(1 + y)^2. \tag{21}$$

The second parameter is related to the tangent of an entrance channel phase (similar to the semiclassical phase at zero collision energy in the model by Gribakin *et al.*[28]) and thus it can vary in the range $\pm\infty$. The model provides analytical expressions in terms of these parameters which can be used to fit experimental data.[103] In particular, under the validity of the model, the value of the reaction rate in a system with $n = 4$ is given by[105]

$$k(E) = \frac{4\bar{a}\pi\hbar}{\mu} \times \frac{y(1 + s^2)}{1 + s^2y^2}, \tag{22}$$

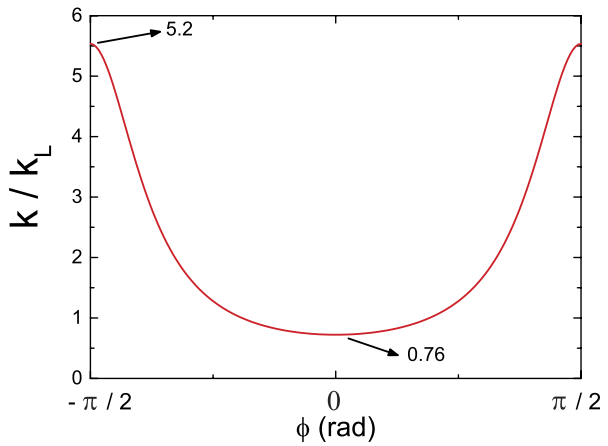

FIG. 11. Values for the rate coefficient in the Wigner limit which are compatible with $P^{\rm re} \approx 0.8$. All the possible values of the parameter $s = \tan\phi$ are considered. Plot as a function of ϕ instead of s is shown.

where μ is the reduced mass of the system. In the same notation, the Langevin rate can be expressed as $k_L(E) = 2\bar{a}\pi\hbar/\mu$ and the result from Eq. (22) in the limit $y = 1$ is twice the Langevin result, $k(E) = 2k_L(E)$, as noted before.

The determination of the y ($P^{\rm re}$) and s parameters for systems complying with the model amounts to characterize its behavior in the ultracold regime completely, as well as in a wide range of collision energies above it.[105] Assuming $P^{\rm re} \approx 0.8$, the value we have got on average in the Langevin region, we obtain $y = 0.38$ and only s needs to be determined to completely characterize the ultracold rate. In Fig. 11, all the values for $k(E)$ which are compatible with $y = 0.38$ through Eq. (22) are shown. To the extent of the validity of the model, this would allow us to bound its value. Therefore, although the QM ultracold reaction rate coefficient, $k(E) \approx 1.1k_L$, is probably affected by the inaccuracies of the PES, the experimental value is likely to be confined in the $0.76k_L < k(E) < 5.2k_L$ range. This reinforces our finding of a mainly constant rate coefficient in the whole considered range.

IV. SUMMARY AND CONCLUSIONS

We have carried out a detailed study of the $D^+ + H_2$ ion-molecule system under the cold and ultracold regimes, covering the 10^{-8}–150 K collision energy range. Rigorous quantum mechanical calculations have been performed on the potential energy surface by Velilla *et al.* (VLABP PES), which faithfully reproduces the long range (quadrupole and charge-induce dipole) behavior. The quantum dynamical methodology used in this work is especially appropriate to calculate *ab initio* cross sections at extremely low collision energies. In addition, the method is ideally suited to tackle complex mediated reactions.

The methodology has been applied to a reactive ion-molecule system governed by a R^{-4} potential at sufficiently large distances. Such a long-range interaction makes the calculations more demanding than other shorter range potential (such as $\sim R^{-6}$) since propagations up to distances on the order of 10^5 a_0 are required. Interpolation methods in the spirit of MQDT are suggested which may lead to a considerable reduction of the computational cost. The calculated elastic and reactive cross sections and rate coefficients have been found to comply with the expected threshold laws.

Interestingly, the absolute value of the rate coefficient and its energy dependence in the ultracold regime are well accounted for by the classical Langevin model, which, in principle, is expected to work only when several partial waves are open. However, such coincidence must be deemed as accidental and would only occur for $n = 4$ potentials. Should this behavior be confirmed by the experiment, a system would have been found with a reaction rate coefficient which remains almost constant in a kinetic energy range of more than ten orders of magnitude. We have analyzed the behavior found in the ultracold regime in terms of the quantum-defect model in Ref. 103. The expressions of the model provide some additional arguments to support the finding of an essentially constant rate coefficient.

ACKNOWLEDGMENTS

We are grateful to A. Aguado for modifying the code of the potential energy surface, making it suitable for the present calculations. The Spanish Ministries of Science and Innovation and Economy and Competitiveness (Grant Nos. CSD2009-00038 and CTQ2012-37404-C02) are gratefully acknowledged.

[1]P. Staanum, S. D. Kraft, J. Lange, R. Wester, and M. Weidemüller, Phys. Rev. Lett. **96**, 023201 (2006).
[2]N. Zahzam, T. Vogt, M. Mudrich, D. Comparat, and P. Pillet, Phys. Rev. Lett. **96**, 023202 (2006).
[3]R. Wynar, R. S. Freeland, D. J. Han, C. Ryu, and D. J. Heinzen, Science **287**, 1016 (2000).
[4]T. Mukaiyama, J. R. Abo-Shaeer, K. Xu, J. K. Chin, and W. Ketterle, Phys. Rev. Lett. **92**, 180402 (2004).
[5]N. Syassen, T. Volz, S. Teichmann, S. Dürr, and G. Rempe, Phys. Rev. A **74**, 062706 (2006).
[6]E. R. Hudson, N. B. Gilfoy, S. Kotochigova, J. M. Sage, and D. DeMille, Phys. Rev. Lett. **100**, 203201 (2008).
[7]S. Ospelkaus, K.-K. Ni, D. Wang, M. H. G. de Miranda, B. Neyenhuis, G. Quéméner, P. S. Julienne, J. L. Bohn, D. S. Jin, and J. Ye, Science **327**, 853 (2010).
[8]A. Canosa, F. Goulay, I. R. Sims, and B. R. Rowe, *Low Temperatures and Cold Molecules* (World Scientific, Singapore, 2008).
[9]C. Berteloite, M. Lara, S. D. L. Picard, F. Dayou, J.-M. Launay, A. Canosa, and I. R. Sims, Faraday Discuss. **142**, 236 (2009).
[10]W. D. Geppert, F. Goulay, C. Naulin, M. Costes, A. Canosa, S. D. L. Picard, and B. R. Rowe, Phys. Chem. Chem. Phys. **6**, 566 (2004).
[11]M. Costes and C. Naulin, Phys. Chem. Chem. Phys. **12**, 9154 (2010).
[12]S. Y. T. van de Meerakker and G. Meijer, Faraday Discuss. **142**, 113 (2009).
[13]P. C. Zieger, S. Y. T. van de Meerakker, C. E. Heiner, H. L. Bethlem, A. J. A. van Roij, and G. Meijer, Phys. Rev. Lett. **105**, 173001 (2010).
[14]K. Dulitz, M. Motsch, N. Vanhaecke, and T. P. Softley, J. Chem. Phys. **140**, 104201 (2014).
[15]A. B. Henson, S. Gersten, Y. Shagam, J. Narevicius, and E. Narevicius, Science **338**, 234 (2012).
[16]Y. Shagam and E. Narevicius, J. Phys. Chem. C **117**, 22454 (2013).
[17]E. Narevicius and M. G. Raizen, Chem. Rev. **112**, 4879 (2012).
[18]Y. Shagam and E. Narevicius, Phys. Rev. A **85**, 053406 (2012).
[19]E. Lavert-Ofir, Y. Shagan, A. B. Henson, S. Gersten, J. Klos, P. Zuchowski, J. Narevivius, and E. Narevicius, Nat. Chem. **6**, 332 (2014).
[20]P. Julienne, Faraday Discuss. **142**, 361 (2009).
[21]H. R. Sadeghpour, J. L. Bohn, M. J. Cavagnero, B. D. Esry, I. I. Fabrikant, J. H. Macek, and A. R. P. Rau, J. Phys. B: At., Mol. Opt. Phys. **33** (2000).
[22]G. Quéméner, N. Balakrishnan, and A. Dalgarno, *Cold Molecules: Theory, Experiment, Applications* (CRC Press, 2009).

[23]T. V. Tscherbul and A. A. Buchachenko, New J. Phys. **17**, 035010 (2015).
[24]M. Tacconi, S. Bovino, and F. A. Gianturco, Phys. Chem. Chem. Phys. **14**, 637 (2012).
[25]T. Roy and S. Mahapatra, Chem. Phys. **448**, 34 (2015).
[26]S. Bovino, M. Tacconi, and F. A. Gianturco, J. Phys. Chem. A **115**, 8197 (2011).
[27]D. de Fazio, Phys. Chem. Chem. Phys. **16**, 11662 (2014).
[28]G. F. Gribakin and V. V. Flambaum, Phys. Rev. A **48**, 546 (1993).
[29]S. D. Smith, Chem. Rev. **92**, 1473 (1992).
[30]E. Herbst, Chem. Soc. Rev. **30**, 168 (2001).
[31]T. P. Snow and V. M. Bierbaum, Annu. Rev. Anal. Chem. **1**, 229 (2008).
[32]R. B. Rowe and J. B. Marquette, Int. J. Mass Spectrom. Ion Processes **80**, 239 (1987).
[33]M. Hawley, T. L. Mazely, L. K. Randeniya, R. S. Smith, X. K. Zeng, and M. A. Smith, Int. J. Mass Spectrom. Ion Processes **97**, 55 (1990).
[34]M. A. Smith, Int. Rev. Phys. Chem. **17**, 35 (1998).
[35]I. W. M. Smith and R. B. Rowe, Acc. Chem. Res. **33**, 261 (2000).
[36]E. Teloy and D. Gerlich, Chem. Phys. **4**, 417 (1974).
[37]D. Gerlich, in *State-selected and state-to-state ion-molecule Reaction Dynamics*, edited by C.-Y. Ng and M. Baer (Advances in Chemical Physics, 1992), Vol. 82, Chap. 1, ISBN 0-471-53258-4.
[38]P. Tosi, Chem. Rev. **92**, 1667 (1992).
[39]D. Gerlich, J. Chem. Soc., Faraday Trans. **89**, 2199 (1993).
[40]D. Gerlich, Phys. Scr., T **59**, 256 (1995).
[41]S. Willitsch, M. T. Bell, A. D. Gingell, and T. P. Softley, Phys. Chem. Chem. Phys. **10**, 7200 (2008).
[42]F. H. J. Hall and S. Willitsch, Phys. Rev. Lett. **109**, 233202 (2012).
[43]S. Willitsch, M. T. Bell, A. D. Gingell, S. R. Procter, and T. P. Softley, Phys. Rev. Lett. **100**, 043203 (2008).
[44]D. Gerlich, R. Plasil, I. Zymak, M. Hejduk, P. Jusko, D. Mulin, and J. Glosík, J. Phys. Chem. A **117**, 10068 (2013).
[45]J. R. Krenos, R. K. Preston, R. Wolfgang, and J. C. Tully, J. Chem. Phys. **60**, 1634 (1974).
[46]D. Gerlich, U. Nowotny, C. Schlier, and E. Teloy, Chem. Phys. **47**, 245 (1980).
[47]D. Gerlich, in *Symposium on Atomic and Surface Physics*, edited by W. Lindinger, F. Howorka, T. D. Märk, and F. Egger (Institut fuer Atomphysik der Universitat Innsbruck, Innsbruck, 1982), p. 304.
[48]C. Schlier and U. Vix, Chem. Phys. **113**, 211 (1987).
[49]M. Berblinger and C. Schlier, J. Chem. Phys. **101**, 4750 (1994).
[50]G. Ochs and E. Teloy, J. Chem. Phys. **61**, 4930 (1974).
[51]F. C. Fehsenfeld, D. L. Albritton, Y. A. Bush, P. G. Fournier, T. R. Govers, and J. Fournier, J. Chem. Phys. **61**, 2150 (1974).
[52]M. J. Henchman, N. G. Adams, and D. Smith, J. Chem. Phys. **75**, 1201 (1981).
[53]H. Villinger, M. J. Henchman, and W. Lindinger, J. Chem. Phys. **76**, 1590 (1982).
[54]D. Müller, Diplom thesis, University of Freiburg, Germany, 1983.
[55]A. Ichihara and K. Yokoyama, J. Chem. Phys. **103**, 2109 (1995).
[56]A. Aguado, O. Roncero, C. Tablero, C. Sanz, and M. Paniagua, J. Chem. Phys. **112**, 1240 (2000).
[57]H. Kamisaka, W. Bian, K. Nobusada, and H. Nakamura, J. Chem. Phys. **116**, 654 (2002).
[58]W. Kutzelnigg and R. Jaquet, Philos. Trans. R. Soc., A **364**, 2855 (2006).
[59]L. P. Viegas, A. Alijah, and A. J. C. Varandas, J. Chem. Phys. **126**, 074309 (2007).
[60]L. Velilla, B. Lepetit, A. Aguado, J. A. Beswick, and M. Paniagua, J. Chem. Phys. **129**, 084307 (2008).
[61]R. A. Bachorz, W. Cenek, R. Jaquet, and J. Komasa, J. Chem. Phys. **131**, 024105 (2009).
[62]T. Takayanagi, Y. Kurosaki, and A. Ichihara, J. Chem. Phys. **112**, 2615 (2000).
[63]T. González-Lezana, A. Aguado, M. Paniagua, and O. Roncero, J. Chem. Phys. **123**, 194309 (2005).
[64]R. F. Lu, T. S. Chu, and K. L. Han, J. Phys. Chem. A **109**, 6683 (2005).
[65]F. J. Aoiz, V. Sáez-Rábanos, T. González-Lezana, and D. E. Manolopoulos, J. Chem. Phys. **126**, 161101 (2007).
[66]F. J. Aoiz, T. González-Lezana, and V. Sáez-Rábanos, J. Chem. Phys. **127**, 174109 (2007).
[67]E. Carmona-Novillo, T. González-Lezana, O. Roncero, P. Honvault, J.-M. Launay, N. Bulut, F. J. Aoiz, L. Bañares, A. Trottier, and E. Wrede, J. Chem. Phys. **128**, 014304 (2008).
[68]C. H. Zhang, W. Q. Zhang, and M. D. Chen, J. Theor. Comput. Chem. **8**, 403 (2009).
[69]W. Q. Zhang and M. D. Chen, J. Theor. Comput. Chem. **8**, 1131 (2009).
[70]T. González-Lenzana, P. Honvault, P. G. Jambrina, F. J. Aoiz, and J.-M. Launay, J. Chem. Phys. **131**, 044315 (2009).
[71]A. Zanchet, O. Roncero, T. González-Lezana, A. Rodíguez-López, A. Aguado, C. Sanz-Sanz, and S. Gómez–Carrasco, J. Phys. Chem. A **113**, 14488 (2009).
[72]P. G. Jambrina, F. J. Aoiz, C. J. Eyles, V. J. Herrero, and V. Sáez-Rábanos, J. Chem. Phys. **130**, 184303 (2009).
[73]W. Zhang, Y. Li, X. Chu, and M. D. Chen, Chem. Phys. **367**, 115 (2010).
[74]P. G. Jambrina, F. J. Aoiz, N. Bulut, S. C. Smith, G. G. Balint-Kurti, and M. Hankel, Phys. Chem. Chem. Phys. **12**, 1102 (2010).
[75]P. G. Jambrina, J. M. Alvariño, F. J. Aoiz, V. J. Herrero, and V. Sáez-Rábanos, Phys. Chem. Chem. Phys. **12**, 12591 (2010).
[76]T. P. Grozdanov and R. McCarroll, J. Phys. Chem. A **115**, 6872 (2011).
[77]M. Tomza, Phys. Rev. Lett. **115**, 063201 (2015).
[78]W. D. Watson, Astrophys. J. **181**, L129 (1973).
[79]D. Gerlich and S. Schlemmer, Planet. Space Sci. **50**, 1287 (2002).
[80]T. J. Millar, Astron. Geophys. **46**, 2.29 (2005).
[81]P. Honvault and Y. Scribano, J. Phys. Chem. A **117**, 13205 (2013).
[82]T. González-Lezana, P. Honvault, and Y. Scribano, J. Chem. Phys. **139**, 054301 (2013).
[83]P. Honvault and Y. Scribano, J. Phys. Chem. A **117**, 9778 (2013).
[84]J.-M. Launay and M. L. Dourneuf, Chem. Phys. Lett. **169**, 473 (1990).
[85]M. Lara, F. Dayou, and J.-M. Launay, Phys. Chem. Chem. Phys. **13**, 8359 (2011).
[86]M. Lara, P. G. Jambrina, F. J. Aoiz, and J.-M. Launay, Phys. Rev. A **91**, 030701 (2015).
[87]L. Bañares, F. Aoiz, P. Honvault, and J.-M. Launay, J. Phys. Chem. A **108**, 1616 (2004).
[88]P. Honvault and J.-M. Launay, J. Chem. Phys. **114**, 1057 (2001).
[89]L. Bañares, J. F. Castillo, P. Honvault, and J.-M. Launay, Phys. Chem. Chem. Phys. **7**, 627 (2005).
[90]P. Honvault and J.-M. Launay, *Theory of Chemical Reaction Dynamics*, NATO Science Series (Kluwer, 2004), Vol. 145.
[91]P. Soldán, M. T. Cvitaš, J. M. Hutson, P. Honvault, and J.-M. Launay, Phys. Rev. Lett. **89**, 153201 (2002).
[92]G. Quéméner, P. Honvault, and J.-M. Launay, Eur. Phys. J. D **30**, 201 (2004).
[93]W. A. Lester, Methods Comput. Phys. **10**, 211 (1971).
[94]M. Lara, J. L. Bohn, D. E. Potter, P. Soldán, and J. M. Hutson, Phys. Rev. A **75**, 012704 (2007).
[95]J. Hazra, B. P. Ruzic, J. L. Bohn, and N. Balakrishnan, Phys. Rev. A **90**, 062703 (2014).
[96]W. Kolos and L. Wolniewicz, J. Chem. Phys. **46**, 1426 (1967).
[97]E. J. Rackham, T. González-Lezana, and D. E. Manolopoulos, J. Chem. Phys. **119**, 12895 (2003).
[98]E. J. Rackham, F. Huarte-Larranaga, and D. E. Manolopoulos, Chem. Phys. Lett. **343**, 356 (2001).
[99]F. J. Aoiz, T. González-Lezana, and V. Sáez-Rábanos, J. Chem. Phys. **129**, 094305 (2008).
[100]R. Côté and A. Dalgarno, Phys. Rev. A **62**, 012709 (2000).
[101]J. Weiner, V. S. Bagnato, S. Zilio, and P. S. Julienne, Rev. Mod. Phys. **71**, 1 (1999).
[102]Z. Idziaszek, A. Simoni, T. Calarco, and P. S. Julienne, New J. Phys. **13**, 083005 (2011).
[103]K. Jachymski, M. Krych, P. S. Julienne, and Z. Idziaszek, Phys. Rev. Lett. **110**, 213202 (2013).
[104]B. Gao, Phys. Rev. A **83**, 062712 (2011).
[105]K. Jachymski, M. Krych, P. S. Julienne, and Z. Idziaszek, Phys. Rev. A **90**, 042705 (2014).
[106]Let us consider, for example, the case $J = 2$. There are three open rovibrational states of HD at the considered collision energies. The incoming channel has quantum numbers ($v = 0$, $j = 0$, $\ell = 2$, $J = 2$), and the total angular momentum, $J = 2$, and the parity, $\epsilon = (-1)^{j+l} = +1$ are conserved in the collision; therefore, the product collision channels which are coupled to the incoming channel are ($v' = 0$, $j' = 0$, $\ell' = 2$, $J = 2$), ($v' = 0$, $j' = 1$, $\ell' = 3$, $J = 2$), ($v' = 0$, $j' = 1$, $\ell' = 1$, $J = 2$), ($v' = 0$, $j' = 2$, $\ell' = 4$, $J = 2$), ($v' = 0$, $j' = 2$, $\ell' = 2$, $J = 2$), ($v' = 0$, $j' = 2$, $\ell' = 0$, $J = 2$). Consequently, there are 7 coupled channels, with $A(E) = 1$ and $B(E) = 6$.
[107]In the simplistic one channel case, this capture probabilities can be numerically calculated for any value of k by propagating inwards the logarithmic derivatives of regular and irregular Bessel functions under the effect of the effective LR potential, and matching at short distance with perfect absorption WKB conditions. The value of these capture probabilities at very low k are found to be $4k\bar{a}$, where $\bar{a}$ is the mean scattering length defined in the text.[103]